

Differential inhibitory effects of resveratrol on excitotoxicity and synaptic plasticity: involvement of NMDA receptor subtypes

Chung-Pin Hsieh, Wei-Tang Chang, Linyi Chen, Hwei-Hsien Chen & Ming-Huan Chan

To cite this article: Chung-Pin Hsieh, Wei-Tang Chang, Linyi Chen, Hwei-Hsien Chen & Ming-Huan Chan (2019): Differential inhibitory effects of resveratrol on excitotoxicity and synaptic plasticity: involvement of NMDA receptor subtypes, *Nutritional Neuroscience*, DOI: [10.1080/1028415X.2019.1641995](https://doi.org/10.1080/1028415X.2019.1641995)

To link to this article: <https://doi.org/10.1080/1028415X.2019.1641995>



Published online: 22 Jul 2019.



Submit your article to this journal [↗](#)



View Crossmark data [↗](#)



Differential inhibitory effects of resveratrol on excitotoxicity and synaptic plasticity: involvement of NMDA receptor subtypes

Chung-Pin Hsieh^a, Wei-Tang Chang^a, Linyi Chen^b, Hwei-Hsien Chen^{b,a,c} and Ming-Huan Chan^{b,c,d}

^aCenter for Neuropsychiatric Research, National Health Research Institutes, Zhunan, Taiwan; ^bInstitute of Molecular Medicine, National Tsing Hua University, Hsinchu, Taiwan; ^cInstitute of Neuroscience, National Chengchi University, Taipei, Taiwan; ^dResearch Center for Mind, Brain and Learning, National Chengchi University, Taipei, Taiwan

ABSTRACT

Objectives: The neuroprotective effects of resveratrol against excitatory neurotoxicity have been associated with N-methyl-D-aspartate receptor (NMDAR) inhibition. This study examined the differential inhibitory effects of resveratrol on NMDAR-mediated responses in neuronal cells with different NMDAR subtype composition.

Methods: The effects of resveratrol on NMDA-induced cell death and calcium influx in immature and mature rat primary cortical neurons were determined and compared. Moreover, the potencies and efficacies of resveratrol to inhibit NR1/NR2A, NR1/NR2B, NR1/NR2C, and NR1/NR2D NMDAR expressed in HEK 293 cells were evaluated.

Results: Resveratrol significantly attenuated NMDA-induced cell death in mature neurons, but not in immature neurons. Resveratrol also concentration-dependently reduced NMDA-induced calcium influx among all NMDAR subtypes, but displayed NR2 subunit selectivity, with a potency rank order of NR2B = NR2D > NR2A = NR2C and an efficacy rank order of NR2B = NR2C > NR2A = NR2D. Data show the stronger inhibitory effects of resveratrol on NR1/NR2B than other subtypes. Moreover, resveratrol did not affect hippocampal long-term potentiation (LTP), but impaired long-term depression (LTD).

Discussion: These findings reveal the specific NMDAR modulating profile of resveratrol, providing further insight into potential mechanisms underlying the protective effects of resveratrol on neurological disorders.

KEYWORDS

Cortical neuron; hippocampus; neurotoxicity; calcium; LTP; LTD; resveratrol; NMDAR subtypes

1. Introduction

N-methyl-D-aspartate receptors (NMDARs) belong to the family of ionotropic glutamate receptors that permit calcium influx and give rise to excitatory synaptic transmission in physiological state and excitotoxicity in neuropathologic condition [1,2]. The molecular structure of NMDARs are heterotetrameric assembly, typically containing two NR1 subunits and other two subunits including NR2 (A, B, C & D) or NR3 (A & B) variants [3]. The various combinations of NR2 subunits produce multiple subtypes of NMDAR. NR2A- and NR2B-containing receptors generate high conductance opening, whereas NR2C- and NR2D-containing receptors have low conductance opening [4]. Expression of the NR2 subunits varies across different brain regions, developmental stages and physiological responses to environmental stimulation [2,5]. Meanwhile, NR2 subtypes provide different physiological function [2,3]. For example, several lines of evidence have indicated that NR2A is involved in cell survival and long-term potentiation (LTP), whereas NR2B activation gives rise to cell death and long-term depression (LTD) [6,7].

Although some controversial observations confer that the differences in NR2 subunit function depend on the receptor location, assemble types, associated signaling cascades and activation amplitude [8–12], the NR2 diversity is indeed involved in pathological conditions and the antagonists for specific NR2 subunits have selective therapeutic effects on distinct neurological disorders [2,5,13]. For instance, hyper-activation or upregulation of NR2B has been suggested to be involved in neurological diseases including stroke, ischemia, chronic pain, Alzheimer's disorder and Huntington's disease [13–16] and the NR2B-selective antagonists have shown to protect against these diseases in animal models [14,17,18]. NR2C- and NR2D-containing NMDARs are critical for ischemia-induced myelin damage which is protected by NR2C/D antagonists [19,20]. In fact, the selective NMDAR antagonists for distinct subtypes have more efficient and lower side therapeutic effects for specific neurological disorders compared to non-selective NMDAR antagonists [21,22]. There is a growing interest in exploiting the pharmacological heterogeneity of NMDAR for development of novel NMDAR subtype selective antagonist that might

provide more efficient implication for the treatment of specific neurological disorders.

Resveratrol is a polyphenolic compound, which is enriched in some fruits such as grapes, cranberries and peanuts and in drinks including red wine and grape juice. Potential beneficial effects of resveratrol have been provided, including anti-oxidant, anti-aging, and anti-inflammatory properties [23]. In preclinical studies, resveratrol has been shown to attenuate the symptoms associated with various neurologic diseases including ischemia, stroke, seizures, Alzheimer's disease, Parkinson's disease and amyotrophic lateral sclerosis (ALS) [24–26]. Meanwhile, resveratrol provides protection against ALS neurotoxicity and increases the therapeutic window of stroke [27,28].

The neuroprotective effects of resveratrol have been associated with the inhibition of glutamate-induced neurotoxicity by reducing calcium influx into neurons through NMDAR [29]. Resveratrol inhibits NMDAR-mediated inward currents in hippocampal neurons, excitatory field potentials in the medial prefrontal cortex and firing frequency in the spinal trigeminal nucleus caudalis [30–32]. Moreover, resveratrol suppresses NMDA-induced seizure responses and neuronal loss [31,33]. However, resveratrol did not alter the baroreflex responses through fetal hypothalamus-pituitary-adrenal (HPA) axis in response to NMDA [34]. It is possible that the involvement of different NMDAR subtypes underlies these discrepancies. It is of importance to reveal the effects of resveratrol on the activity of NMDAR subtypes.

In this study, we examined the inhibitory effects of resveratrol on NMDAR-induced cell death and calcium influx in immature and mature primary cultured cortical neurons that vary in NMDAR subtype composition. The inhibitory effects of resveratrol on NMDA-elicited calcium influx were further compared among HEK293 cells co-expressing NR1 with different NR2 subunits. Finally, the effects of resveratrol on NMDAR-dependent synaptic plasticity, LTP and LTD, were performed in the hippocampus. The results displayed a unique profile of resveratrol in NMDAR inhibition and shed light on the mechanisms involved in its therapeutic potential in neurological disorders.

2. Materials and methods

2.1. Primary cortical neuron cultures

Cortical neuron cultures were prepared as previously described [31]. Pregnant Sprague-Dawley rats were purchased from BioLASCO Taiwan Co. Ltd (Taiwan). Cortices were dissected from embryo at 18th day of gestation. Tissues were incubated with papain (10 units/mL) for

10 min at 37°C and then dissociated by glass pipette. Dissociated cells were passed through a 70 µm strainer and washed twice with PBS. Cells were then seeded on 0.2 mg/mL poly-L-ornithine (Sigma-Aldrich)-coated coverslips or plates. On day *in vitro* (DIV) 0, cells were cultured in minimum essential media/high glucose medium (GIBCO) supplemented with 5% fetal bovine serum (FBS, Biological Industry), 5% horse serum, 0.5 mg/mL penicillin and streptomycin (GIBCO) under 37°C and 5% CO₂ conditions. On DIV 1, the culture medium was replaced with Neurobasal medium supplemented with B27, 2 mM glutamine, 1 × Antibiotic-Antimycotic (NB/B27, GIBCO) containing 25 µM glutamate to induce neurite growth. On DIV 2, the medium was replaced with NB/B27 containing 3.5 µM cytosine-1-β-D-arabinofuranoside to inhibit the growth of glial cells. After DIV 3, cells were routinely maintained in NB/B27 culture medium, and half volume of medium was replaced with fresh medium each 2 d. Cortical neurons at DIV 7–9 and DIV 14–16 were identified as immature and mature stage, respectively [35].

2.2. MTT assay

The procedure of 3-(4,5-dimethylthiazol-2-yl)-2,5-diphenyl tetrazolium bromide (MTT) assay was modified from that described by Schubert and Piasecki [36]. The primary cultured cortical neurons (5×10^4 cells/well) were seeded in 96 well plates to measure NMDA-induced neuronal death at DIV 7 or 14. Firstly, cultured cells were washed with HEPES-buffered salt solution (HCSS) containing (in mM) 120 NaCl, 5.4 KCl, 1.8 CaCl₂, 15 D-glucose, and 20 HEPES, pH 7.4. Immediately thereafter, cells were incubated with DMSO (vehicle, 0.1%), resveratrol (0.1, 1, and 10 µM, Sigma-Aldrich) or MK-801 (10 µM, Tocris Bioscience) for 15 min and then added with NMDA (30 µM, Sigma-Aldrich) plus glycine (10 µM, J.T. Baker) for 15 min. Then the reaction was terminated by replacement of the NB/B27. After 24 h, MTT (0.5 mg/mL, Sigma-Aldrich) was applied to the treated cells at 37°C for 3 h. The culture medium was then removed and 100 µL DMSO was added to each well. After 10 min, absorption values at 570 and 630 nm were measured with an ELISA reader (Molecular Devices). The relative cell viability was represented as the intensity value of 630 nm subtracted from 570 nm and then normalized to the average of vehicle control.

2.3. Establishment of stable cell lines expressing NMR subtypes

2.3.1. Plasmid constructs

Full length human *GRIN1*, *GRIN2A*, *GRIN2B*, *GRIN2C* and *GRIN2D* cDNA were amplified using template

from the plasmid DNAs, pCDNA/Hygro(-) individually containing human *GRIN1*, *GRIN2A*, *GRIN2B* and *GRIN2C* cDNA which were generously provided by Dr. Chia-Hsiang Chen (Chang Gung Memorial Hospital). The amplified *GRIN1* DNA fragment was infused into pLKO-AS3W.puro vector (National RNAi Core Facility, Academia Sinica, Taipei, Taiwan), and *GRIN2A*, *GRIN2B* and *GRIN2C* fragments were individually infused into pLKO-AS3W.neo vector (National RNAi Core Facility, Academia Sinica, Taipei, Taiwan). *GRIN2D* cDNA tagged with green fluorescence protein (GFP) cDNA in pCMV6-AC-GFP plasmid DNA (AMS Biotechnology) was also provided by Dr. Chen. Infusions were performed according to instructions provided with the In-Fusion@ HD cloning kit (Takara Bio INC). All constructs were validated by DNA sequencing.

2.3.2. Lentivirus production

Recombinant lentivirus was prepared according to the protocol provided by the National RNAi Core Facility. Triple transfection with the gag-pol-rev packaging plasmid (pCMV Δ R8.91), the env plasmid encoding VSV glycoprotein (pMD.G) and the expressing vectors pLKO-AS3W.puro containing *GRIN1* cDNA or pLKO-AS3W.-neo containing *GRIN2A*, *GRIN2B* and *GRIN2C* cDNA were performed in HEK293FT cells (Invitrogen) using transIT@-LT1 (Mirus Bio). Lentivirus particles in growth medium (Dulbecco's Modified Eagle Medium, DMEM) supplemented with 10% FBS and 0.05 mg/mL penicillin and streptomycin were collected after incubation for 48 and 72 h and stored at -80°C .

2.3.3. Generation of stable cell lines

A stable cell line expressing NR1 was first established. HEK293 cells (Bioresource Collection and Research Center, Hsinchu, Taiwan) were cultured in growth medium supplemented with polybrene (8 $\mu\text{g}/\text{mL}$) and infected with lentivirus containing *GRIN1* cDNA for 24 h. The infection procedure followed the protocol from the National RNAi Core Facility. Viruses were removed and cells were incubated with growth medium supplemented with 2 $\mu\text{g}/\text{mL}$ puromycin for 72 h. Viable single cells were then transferred to individual wells of a 96 well plate and incubated with growth medium supplemented with 2 $\mu\text{g}/\text{mL}$ puromycin for 7 d. Clones expressing NR1 were selected and confirmed by constitutive expression of NR1 protein for more than 5 generations (data not shown). Stable cell lines were routinely maintained in growth medium supplemented with 0.5 $\mu\text{g}/\text{mL}$ puromycin.

Stable cell lines expressing NR1 were then individually infected with lentiviral particles containing *GRIN2A*, *GRIN2B* and *GRIN2C* cDNA for 24 h. Infected

cells were selected by incubation in growth medium supplemented with 0.5 $\mu\text{g}/\text{mL}$ puromycin, 100 $\mu\text{g}/\text{mL}$ G418 (Sigma-Aldrich), 2 mM MgCl_2 and 30 μM MK-801 for 14 d. Surviving cells were then passaged for more than 3 generations. Viable cells constitutively expressing NR1/NR2A, NR1/NR2B or NR1/NR2C were identified by Western blotting. Stable cell lines were maintained in growth medium supplemented with 0.5 $\mu\text{g}/\text{mL}$ puromycin and 20 $\mu\text{g}/\text{mL}$ G418 for selection and 2 mM MgCl_2 and 30 μM MK-801 for preventing excitotoxicity.

2.3.4. Generation of HEK293 expressing NR1/NR2D

Stable cell lines expressing NR1 (6×10^5 cells) were seeded in 6 cm dish and maintained for 24 h. Transient transfection of 2 μg pCMV6-AC-GFP containing *GRIN2D* cDNA was performed using transIT@-LT1 (Mirus Bio). After 24 h, cells (5×10^4 cells) were then seeded on coverslips (18 mm in diameter) and incubated with growth medium supplemented with 0.5 $\mu\text{g}/\text{mL}$ puromycin, 2 mM MgCl_2 and 30 μM MK-801 for 3–5 d. GFP-positive cells were obtained and chosen to record intracellular calcium by calcium image or verify the NR2D expression by immunofluorescence.

2.3.5. Intracellular calcium recording

Primary cortical neurons or HEK293 cells were seeded on 0.2 mg/mL poly-L-ornithine coated 18 mm diameter coverslips. The cortical neurons (4×10^5 cells) cultured at DIV 7–9 or 14–16 were incubated with the Ca^{2+} -indicator fura-2 acetoxymethyl ester (Fura-2 AM, 2 μM , Sigma-Aldrich) in physiological saline containing (in mM) 140 NaCl, 3.5 KCl, 0.4 KH_2PO_4 , 0.33 Na_2HPO_4 , 10 D-Glucose, 10 HEPES and 2.2 CaCl_2 , pH7.4 for 1 h. HEK293 cells (5×10^4 cells) at DIV 3–5 were incubated with 5 μM Fura-2 AM in physiological saline supplemented with 0.02% probenecid and 2 mM MgCl_2 for 1 h. Cells were then washed with physiological saline and incubated for 15 min. Coverslips were moved to perfusion chambers and placed on the stage of an inverted fluorescence microscope (DM IL LED, Leica) equipped with a 40 \times fluorescence oil objective lens (HC PL APO, Leica) for Ca^{2+} -imaging recording.

Regions of interest were selected by drawing around viable cells in NR1/NR2A, NR1/NR2B or NR1/NR2C stable cell lines or GFP-positive cells in cells expressing NR1/NR2D. Dual excitation 340 and 380 nm lights were provided by illuminator shutter (Lambda LS, Shutter Instrument), equipped with a Fura-2 filter wheel controlled by an optical filter changer (Lambda 10-B, Shutter Instrument). Fura-2 intracellular calcium measurements were performed using a video-based digital calcium imaging system set up for dual excitation at 340 and 380 nm and emission at 510 nm. Images were collected and

stored every 2 s with the image-acquisition program, MetaFluor Fluorescence Ratio Imaging Software (Molecular Devices). Results of intracellular calcium analysis were presented as the ratio of fluorescent intensities obtained from 340 nm normalized to 380 nm images.

Cells were continuously perfused with physiological saline using a perfusion valve control system (Warner Instrument). Additional 0.3 μM tetrodotoxin (Abcam) supplement in physiological saline was used in cortical neurons. In cortical neurons, sequential perfusion of resveratrol (0, 0.1, 1, 10 or 100 μM , in 0.1% DMSO) for 60 s was followed by 3 μM NMDA and 10 μM glycine for 40 s. In HEK293 cells, perfusion of resveratrol (0, 0.3, 1, 3, 10, 30 or 100 μM), PEAQX, RO 25-6981, or QNZ46 (1, 1, 5 μM ; Tocris Bioscience) for 60 s was followed by NMDA (10 μM) plus glycine (10 μM) for 40 s. Each treatment was separated by washing with physiological saline for at least 2 min. NMDA-induced changes in intracellular calcium level ($\Delta[\text{Ca}^{2+}]_i$) were quantified by the basal value of F340/380 (F_b) subtracted from the maximum value of F340/380 (F_{max}). All values of $\Delta[\text{Ca}^{2+}]_i$ under resveratrol pretreatment were then normalized to $\Delta[\text{Ca}^{2+}]_i$ of vehicle control.

Concentration-inhibition curves were constructed by fitting data with variable slopes as the following equation:

$$Y = \text{Bottom} + (\text{Top} - \text{Bottom}) / (1 + 10^{((\text{Log}IC_{50} - X) \times \text{Hillslope}))}$$

where Y is $\Delta[\text{Ca}^{2+}]_i$ value, Bottom and Top is minimum and maximum value of $\Delta[\text{Ca}^{2+}]_i$, X is resveratrol concentration to log, and IC_{50} is the value of resveratrol concentration at which the $\Delta[\text{Ca}^{2+}]_i$ is 50% inhibited. The calculation was performed by using GraphPad prism 6.0 software.

2.3.6. Western blotting

HEK293 cells and stable cell lines containing NMDAR subtypes (5×10^5 cells in 6 cm dish) were maintained for 4 d and then collected and dissolved in ice-cold lysis buffer containing (in mM) 100 NaCl, 50 Tris-HCl, 1 EGTA, 1 EDTA, 1% NP-40, pH 7.6, supplemented with protease and phosphatase inhibitor cocktail (Thermo Fisher Scientific). Cells were repeatedly vortexed and immersed in ice for 15 s over the course of 3 min, then incubated on ice for an additional 5 min. Cell lysate was then centrifuged at 14,000g for 20 min and the supernatant was collected. Protein concentrations were quantified with BCA Protein Assay Reagent (Thermo Fisher Scientific).

Proteins in NuPAGE[®] LDS sample buffer supplemented with a reducing agent (Thermo Fisher

Scientific) were heated at 70°C for 10 min. Proteins were separated by 7.5% SDS-polyacrylamide gel electrophoresis for 2 h at 100 V and transferred to PVDF membrane at 100 V for 100 min. The membranes were blocked with 5% dry fat-free milk in PBS containing 0.05% Tween 20 (PBST) for 1 h and incubated overnight with primary antibodies including rabbit monoclonal anti-NR1 (1:1000, Cell Signaling), rabbit polyclonal anti-NR2A (1:1000, Cell Signaling), rabbit monoclonal anti-NR2B (1:1000, Cell Signaling), rabbit monoclonal anti-NR2C (1:1000, Abcam), and mouse monoclonal anti- β -actin (1:5000, Novus) at 4°C. After washing with PBST, the membranes were incubated with horseradish peroxidase-linked secondary antibodies: anti-rabbit IgG (1:5000, Cell Signaling) or anti-mouse IgG for (1:5000, Jackson Laboratory) for 1 h. ECL detection kit (Thermo Fisher Scientific) was then added to produce a chemiluminescence signal which was detected using a cooled CCD camera and digital imaging (UVP imaging system, Thermo Fisher Scientific).

2.3.7. Immunofluorescence

NR1 stable cell line with NR2D transfection was fixed in 4% paraformaldehyde in PBS for 10 min. After washing with PBS, cells were blocked using 5% bovine serum albumin (BSA) and 0.02% Triton X-100 in PBS for 1 h. Cells were incubated with primary goat anti-NR2D polyclonal antibody (1:200, Santa Cruz) in PBS containing 2% BSA and 0.02% Triton X-100 for 16 h at 4°C. Cells were then incubated with rabbit anti-goat IgG antibody conjugated with Alexa Fluor 595 (4 $\mu\text{g}/\text{mL}$, Molecular Probes) for 1 h, counterstained with 1 $\mu\text{g}/\text{mL}$ Hoechst 33258 (Invitrogen) for 1 h and then mounted on slides by using VECTASHIELD[®] Antifade mounting medium (Vector Laboratories). Images were observed and captured using a fluorescence microscope (DM IL LED, Leica) controlled by Metamorph software (Molecular Devices).

2.3.8. Multielectrode array recordings

Brain slice preparations were performed as previously described (31) with slight modifications. Brains from ICR mice (8–12 weeks of age) were dissected and immersed in ice-cold artificial cerebrospinal fluid (ACSF) with the following composition (in mM): 128 NaCl, 1.9 KCl, 2.2 CaCl_2 , 2.0 MgCl_2 , 26 NaHCO_3 , 1.2 KH_2PO_4 and 10 D-glucose, pH 7.38 bubbled with a mixture of 95% O_2 /5% CO_2 . Coronal slices (400 μm) were immediately cut from the hippocampus (1.2–2.8 mm posterior to bregma) using a vibratome (VT1000S, Leica). Slices were recovered by incubation of ACSF saturated with O_2 at 35°C for at least 1 h. The slices were individually transferred to the center area of coated

MED probe (Alpha MED Scientific Inc.), and the pyramidal layer and stratum radiatum of CA1 were positioned to cover the 8×8 microelectrode array by a paint brush. The MED probe is a 64 planar micro-electrode array, and the size of micro-electrode is $50 \times 50 \mu\text{m}^2$. The interpolar distance between probes is 150 or 300 μm . Before initial probe use, the surface of the probe was coated with 0.1% polyethylenimine in 25 mM borate buffer for 16 h at room temperature for efficient adhesion of brain slices to the probe. The slice was then mounted on nylon mesh and slice anchor (Alpha MED Scientific Inc.) to prevent flotation.

For electrophysiological recording, the MED probe was mounted by perfusion cap (MED-KCAP01, Alpha MED Scientific Inc.) and assembled in a perfusion pipe holder kit (Alpha MED Scientific Inc). Continuous perfusion (2 mL/min) of ACSF bubbled with a mixture of 95% O_2 /5% CO_2 at 35°C was passed through the perfusion cap into the probe. Voltage signals were amplified and digitized at 20 kHz (SU-MED640, Alpha MED Scientific Inc). Field excitatory post-synaptic potentials (fEPSPs) in CA1 were evoked by bipolar electrical stimulation (0.1 ms duration) at Schaffer collaterals through one of the electrodes placed in the stratum radiatum. Recording channels 150 or 300 μm from the stimulation site were selected and observed. For LTP and LTD observation, stimulation currents that induce 1/3 (60–80 μA) and 2/3 (100–120 μA) of the maximum amplitude were individually used. The stimulation test under ACSF perfusion was first performed for at least 15 min with 1 min interval until the fEPSP slope was stable and DMSO (0.1%) or resveratrol (0.01, 0.1 and 100 μM) was then alternatively perfused for 10 min. High-frequency stimulation (HFS; 100 Hz, 1s) and low-frequency stimulation (LFS; 1 Hz, 15 min) were used to induce LTP and LTD, respectively. Slice was returned to ACSF perfusion and test stimulation was performed again for 1 h.

Data were obtained and saved using NI-DAQmx14.0 software (Alpha MED Scientific Inc). Digital filtering and the initial slope of fEPSP measurement were then performed using pCLAMP10 software (Molecular Devices). The degree of LTP or LTD was evaluated by normalizing to the mean slope during the last 10 min of baseline under ACSF perfusion before HFS or LFS. The mean slope value over 2 min were averaged and presented. The average normalized slopes from the 51–60 min after induction were quantified and compared.

2.3.9. Statistical analysis

Data are shown as mean \pm SD. Unpaired Student's t-test was used comparing the results from intracellular calcium or LTP measurements. One-way analysis of variance (ANOVA) was used in the MTT assay and some

data from calcium image. Two-way mixed-design ANOVAs with the resveratrol or time as within-subject factor were individually used in calcium image or LTP and LTD results. The *post-hoc* Student–Newman–Keuls multiple comparison tests were selected following with ANOVA test. The level of statistical significance was set at $p < .05$.

3. Results

3.1. Differential neuroprotective effects of resveratrol on NMDA-induced excitotoxicity in immature and mature neurons

The cultured cortical neurons at DIV 7 (immature neuron) and DIV 14 (mature neuron) were challenged with NMDA to induce cell death (Figure 1). Under transient exposure of NMDA/glycine for 15 min and 24 h after NMDA/glycine washout, the cell viability in neurons was reduced to $52.27 \pm 3.20\%$ at DIV 7. The cell viability at DIV 14 became lower and was decreased to $41.66 \pm 2.08\%$. The neuronal cell death induced by NMDA was almost completely protected by pretreatment of non-competitive NMDAR antagonist MK801. In DIV 7 neurons, pretreatment of resveratrol (0.1, 1, and 10 μM) was ineffective for NMDA-induced neurotoxicity (Figure 1(A)). However, resveratrol at 1 and 10 μM , but not 0.1 μM , could significantly reduce NMDA-induced cell death in mature neurons at DIV 14 (Figure 1(B)). In addition, there was no difference in cell viability between treatment with resveratrol (0.1–10 μM) alone and vehicle control.

3.2. Differential inhibitory effects of resveratrol on NMDA-evoked calcium influx in immature and mature neurons

NMDA-evoked calcium influx was higher at DIV 14–16 compared to those at DIV 7–9 (Figure 2). The inhibitory effects of different concentration of resveratrol (0.1, 1, 10 and 100 μM) on NMDA-induced calcium influx were further compared between DIV 7–9 and 14–16 (Figure 2). As shown in Figure 2(D), two-way mixed-design ANOVA with resveratrol as within-subject factor showed significant effect of *resveratrol* ($F_{(1, 39)} = 35.07$, $p < .001$), *culture day* ($F_{(4, 156)} = 125.8$, $p < .001$) and *culture day* \times *resveratrol* interaction ($F_{(4, 156)} = 7.995$, $p < .001$). The Student–Newman–Keuls post hoc test showed the significantly reduced percentage of calcium influx under pretreatment of resveratrol from 0.1 to 100 μM at DIV 7–9 and 14–16. Meanwhile, a significantly lower level of calcium change was observed under resveratrol treatment in each concentration at DIV 14–16.

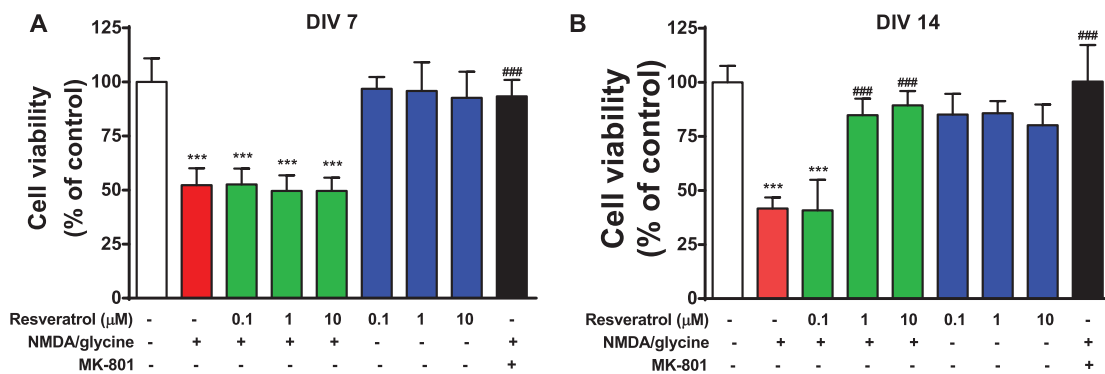


Figure 1. Effects of resveratrol on NMDA-induced cell survival in immature and mature neurons. The primary rat cortical neurons at DIV 7 (A) and DIV 14 (B) were incubated with resveratrol (0.1–10 μM) or MK-801 (10 μM) for 15 min. NMDA/glycine (30/10 μM) were then added to induce neurotoxicity for 15 min. Cells were washed and then maintained for 24 h. Cell viability was determined by MTT assay. Values are mean ± SD ($n = 6$ wells); *** $p < .001$ compared with vehicle control and ### $p < .001$ compared with NMDA/glycine group.

3.3. Characterization of HEK293 cells expressing different types of NMDAR subunits

Western blotting identified the immunosignal of NR1 in stable cell lines expressing human NR1/NR2A, NR1/NR2B and NR1/NR2C, but not in naïve HEK293 cells. NR2A, NR2B and NR2C signals were only detected in cells expressing NR1/NR2A, NR1/NR2B and NR1/NR2C, respectively (Figure 3(A)). NR2D, detected by immunofluorescence, was colocalized with the GFP signal but was not observed in GFP-negative cells (Figure 3(B)).

The function of NMDAR subtypes was determined by measuring the calcium influx in response to NMDA plus glycine. NMDA-induced calcium influx was discriminative among HEK293 cells expressing NR1 with distinct NR2 subtypes. Higher levels of NMDA-induced calcium influx were observed in NR1/NR2A and NR1/NR2B, whereas lower levels occurred in NR1/NR2C and NR1/NR2D (Figure 3(C)). The NMDAR-mediated calcium influx was selectively reduced by the specific NMDAR subtype antagonists (Figure 3(D–H)) for NR2A (PEAQX), NR2B (RO 25-6981), and NR2C/D (QNZ46) in NR1/NR2A- (Figure 3(E)), NR1/NR2B- (Figure 3(F)), NR1/NR2C- (Figure 3(G)) and NR1/NR2D- (Figure 3(H)) expressing cells, respectively, but not affected by other subtype selective antagonist.

3.4. Differential inhibitory effects of resveratrol on NMDA-evoked calcium influx in HEK293 cells expressing different subtypes of NMDAR

The sensitivity of NMDAR-mediated calcium influx in response to resveratrol (0.3, 1, 3, 10, 30, and 100 μM) in HEK293 cells expressing different subtypes of

NMDAR was assessed (Figure 4). Resveratrol (100 μM) has greater inhibitory efficacy for NR1/NR2B (Figure 4(C)) and NR1/NR2C (Figure 4(D)) and lower efficacy for NR1/NR2A (Figure 4(B)) and NR1/NR2D (Figure 4(E)). Meanwhile, the IC_{50} value ranking of resveratrol for the NMDAR subtypes was NR2B = NR2D < NR2A = NR2C (Table 1). The potency of resveratrol to inhibit four NR2 subtypes has up to 24.6-fold difference. NR1/NR2B are the most sensitive subtype to the inhibitory effects of resveratrol.

3.5. Effects of resveratrol on LTP and LTD induction in hippocampal slices

The effects of resveratrol on LTP induction were examined by perfusion of resveratrol at a high concentration (100 μM) during HFS (Figure 5(A–C)). Two-way mixed-design ANOVA with time as a within-subject factor showed a significant main effect of time ($F_{(39, 234)} = 8.226$, $p < .001$) in fEPSP slopes. LTP was successfully induced by HFS in both groups (Figure 5(B)). There was no difference of averaged fEPSP slopes for the last 10 min LTP recording under resveratrol treatment (Figure 5(C)).

Resveratrol (0.01 and 0.1 μM) was perfused during LFS-induced LTD (Figure 5(D–F)). Two-way mixed-design ANOVA with time as a within-subject factor showed significant effects of resveratrol ($F_{(2, 9)} = 8.982$, $p < .01$), time ($F_{(39, 351)} = 8.877$, $p < .001$) and resveratrol × time interaction ($F_{(78, 351)} = 2.970$, $p < .001$) in fEPSP slopes. As shown in Figure 5(E), the reduced slopes were observed after LFS induction. Resveratrol at 0.1 μM, but not at 0.01 μM, significantly attenuated the reduced fEPSP slopes. The reduced average fEPSP slopes for the last 10 min LTD recording in vehicle control was

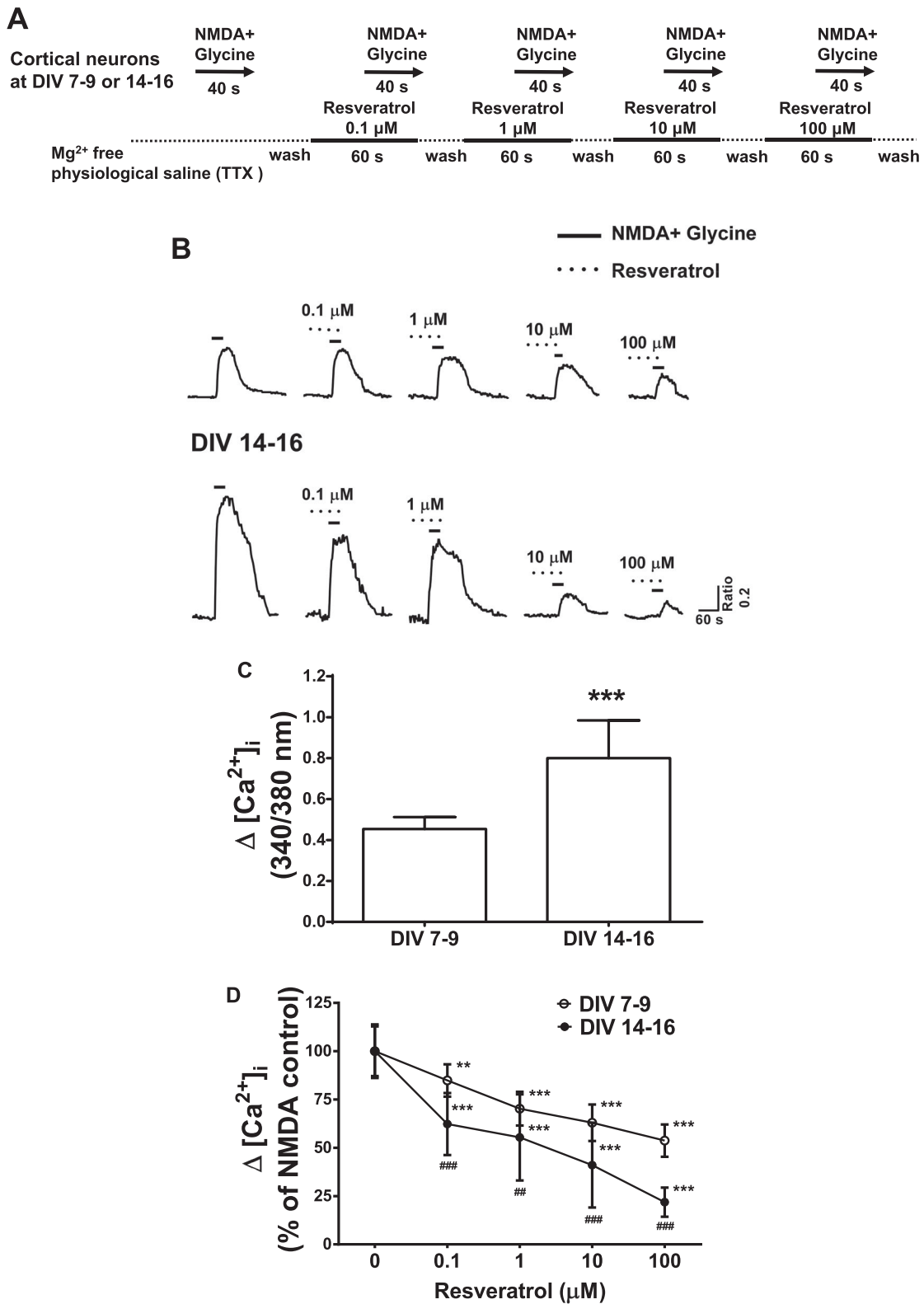


Figure 2. Effects of resveratrol on NMDAR-mediated intracellular calcium signaling in immature and mature neurons. Experimental protocol (A) and representative traces (B) showed NMDA-induced calcium influx in primary cortical neurons at DIV 7-9 and DIV 14-16 that were sequentially perfused with different concentrations of resveratrol (0.1–100 μM) for 60 sec followed by combination of NMDA/glycine (10/10 μM) for 40 sec. Each treatment was separated by physiological saline wash for more than 2 min. (C) NMDA-induced calcium changes ($\Delta[\text{Ca}^{2+}]_i$) were different at DIV 7-9 ($n = 15$ cells) and DIV 14-16 ($n = 26$ cells). $***p < .001$ compared with DIV 7-9. (D) The effects of resveratrol on NMDA-induced $\Delta[\text{Ca}^{2+}]_i$ at DIV 7-9 and DIV 14-16 were quantified and normalized with NMDA/glycine control. Values are mean \pm SD. $**p < .01$ and $***p < .001$ compared with NMDA/glycine control and $##p < .01$ and $###p < .001$ compared between DIV 7-9 and DIV 14-16 at the same concentration of resveratrol.

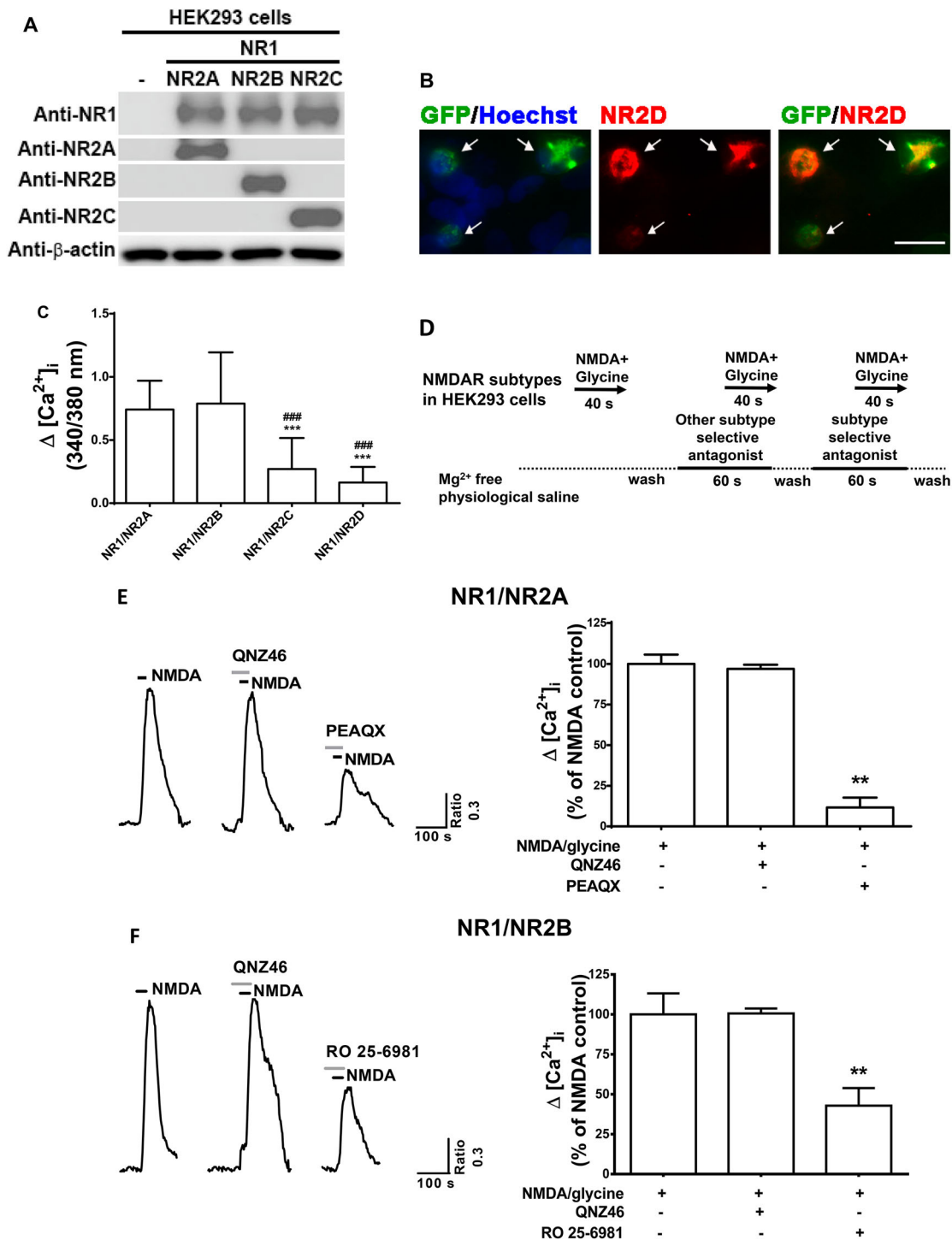


Figure 3. Characterization of NMDAR subtype expression in HEK293 cells. (A) Western blotting analysis demonstrated the immunosignals of NR1, NR2A, NR2B and NR2C among naïve, NR1/NR2A, NR1/NR2B and NR1/NR2C HEK293 stable cell lines. β -actin was used as internal control. (B) NR1 stable cell line was transiently transfected with plasmid DNA containing NR2D-EGFP cDNA. Cells were immunostained with anti-GFP (green) and anti-NR2D (red) antibodies and counterstained with Hoechst 33258 (blue). Arrows indicated the GFP/NR2D-positive cells. Scale bar, 25 μ m. (C) NMDA/glycine (10/10 μ M)-evoked calcium influx among NR1/NR2 variants were quantified ($n = 41, 30, 87, 25$ cells). *** $p < .001$ compared with NR1/NR2A; ### $p < .001$ compared with NR1/NR2B. (D) Experimental protocol and (E–H) representative graphs in left panels showed the pre-perfusion of selective NMDAR subtype antagonists, including PEAQX (1 μ M), RO 25-6981 (1 μ M) and QNZ46 (5 μ M), and right panels showed the NMDA/glycine-evoked calcium changes in HEK293 cells expressing NR1/NR2A ($n = 13$ cells), NR1/NR2B ($n = 18$ cells), NR1/NR2C ($n = 20$ cells), and NR1/NR2D ($n = 14$ cells). Values are mean \pm SD. ** $p < .01$ and *** $p < .001$ compared with NMDA/glycine treatment.

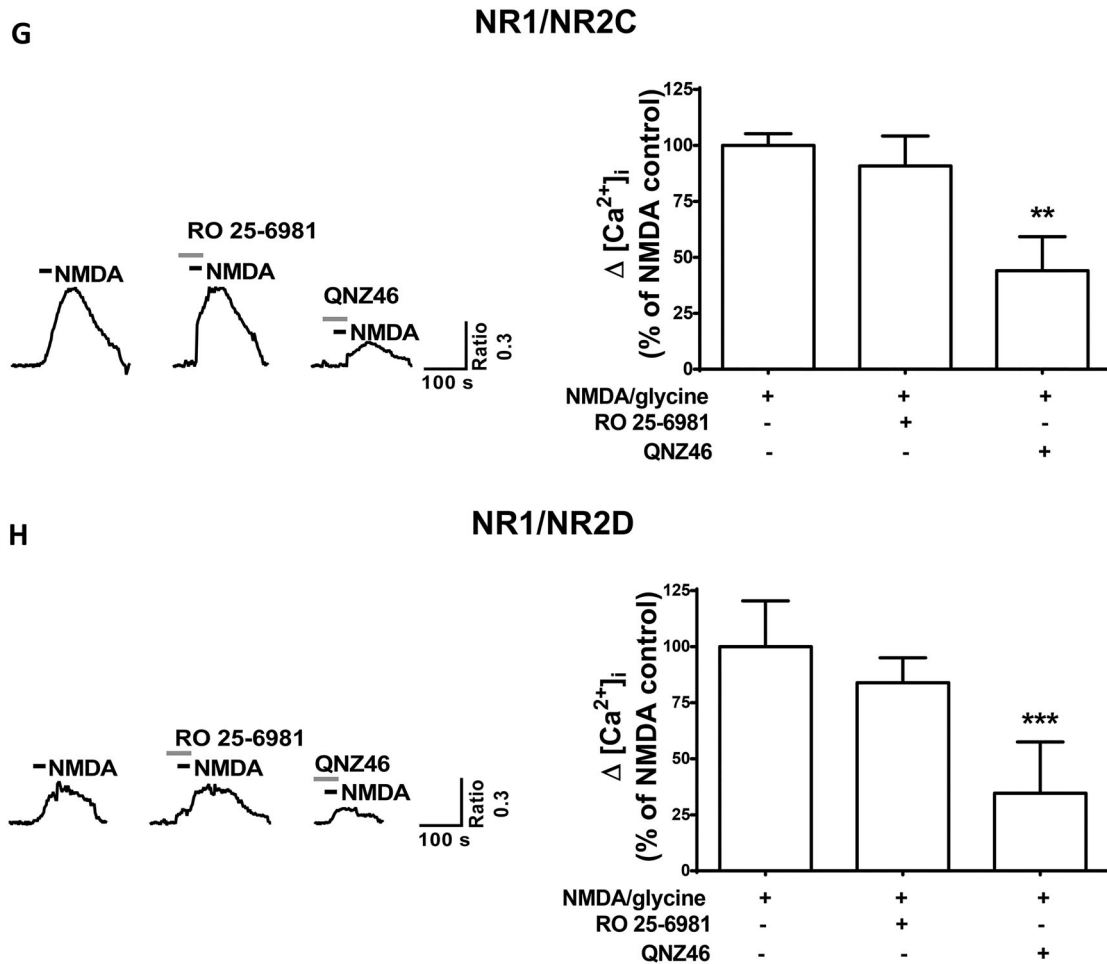


Figure 3 Continued

significantly reversed by resveratrol at 0.1 μ M, but not at 0.01 μ M (Figure 5(F)).

4. Discussion

The present study demonstrated that resveratrol has distinct inhibitory effects on NMDA-induced neuronal death in immature and mature cultured cortical neurons, correlated with NMDA-induced calcium influx. Further investigation of the effects of resveratrol on NMDARs comprised of different NR2 subunits displayed the highest inhibitory potency and efficacy on NMDA-induced calcium influx in NR2B-containing NMDARs. Moreover, resveratrol selectively reduced the induction of NMDAR-dependent LTD, but not LTP in the hippocampus, which was similar to those observed in NR2B subtype-selective antagonists [37]. These results revealed that resveratrol inhibits NMDARs, acting preferably on NR2B subunits.

Previous reports indicate that mature cortical neurons are more sensitive to NMDA-induced toxicity [38,39]. Consistently, our results show the increased NMDA-

dependent calcium influx and a stronger inhibitory effect on this parameter in resveratrol-treated mature neurons, enhancing cell survival after excitotoxic stimulation. The cell death was almost completely abolished by MK-801 in both stages. Concomitant with the developmental changes in the composition of NMDAR, the disparities of immature and mature neurons in response to the protective effects of resveratrol might be attributed to their NMDARs that contain different NR2 subunits.

Resveratrol may alter sodium channel and multiple calcium channels, permitting extracellular and intracellular calcium response [40,41]. In order to avoid membrane depolarization-induced activation of NMDAR, tetrodotoxin was used to block sodium channel and membrane depolarization. Thus, the contribution of calcium influx through voltage-gated calcium channels (VGCCs) linked to membrane depolarization may be partly inhibited under NMDAR-mediated calcium influx. Although VGCCs in the plasma membrane regulated by resveratrol [41] could not be excluded in cortical neurons, calcium influx and cell death induced by strong activation of VGCCs are much less than

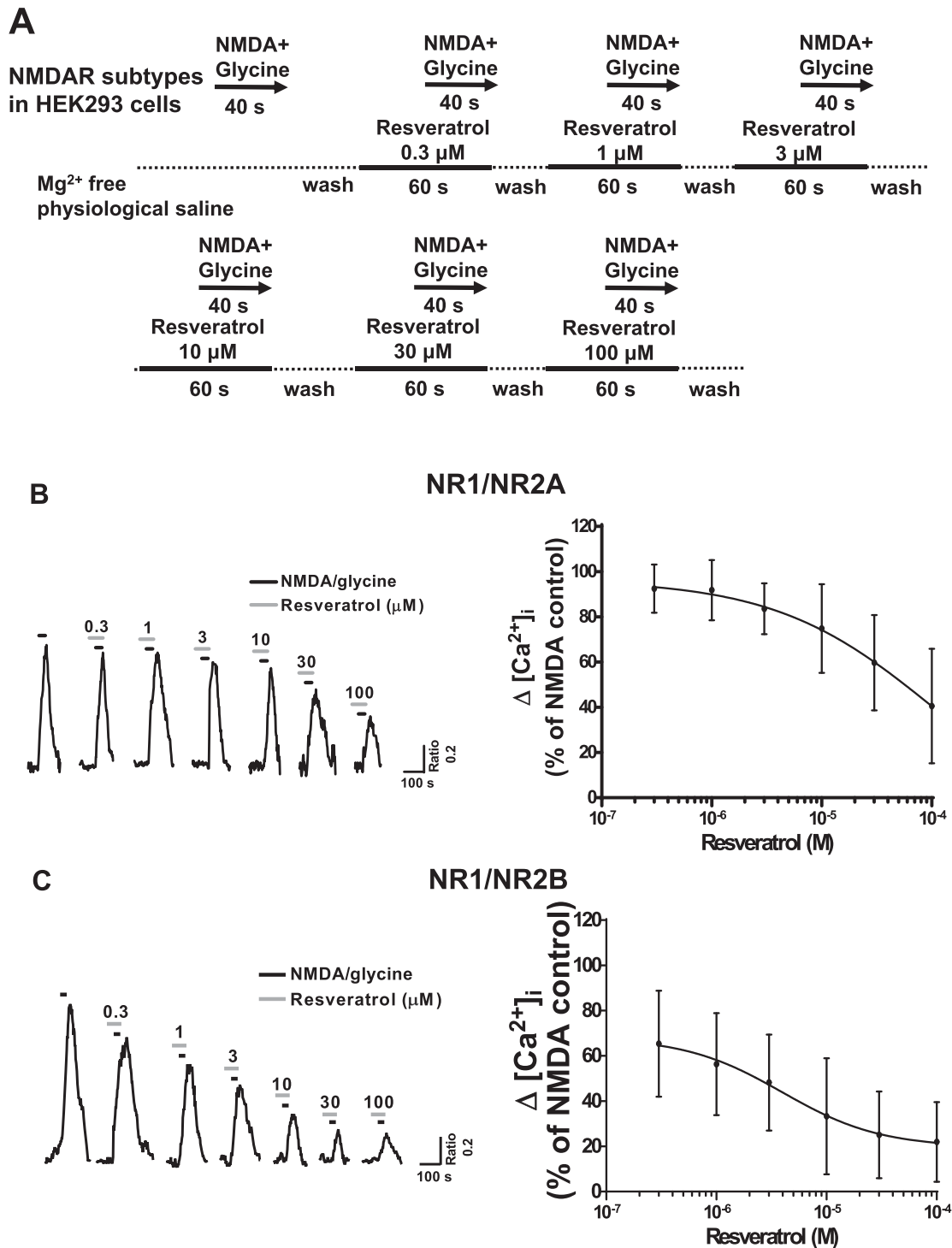


Figure 4. Inhibitory effects of resveratrol on NMDA-evoked intracellular calcium level among NMDAR subtypes in HEK293 cells. Effects of resveratrol on NMDA/glycine-induced intracellular calcium elevation were determined in HEK293 cells expressing NR1/NR2A, NR1/NR2B, NR1/NR2C and NR1/NR2D. (A) Experimental protocol was illustrated. (B–E) Representative traces in left panels showed the sequential perfusion of resveratrol at different concentration (0.3–100 μM) for 60 s followed by NMDA (10 μM)/glycine (10 μM). Different treatments were separated by physiological saline wash for more than 2 min. NMDA-induced $\Delta[Ca^{2+}]_i$ was normalized with NMDA/glycine treatment. In right panels, graphs showed the fitted curves through the mean data obtained from individual cells containing NR1/NR2A ($n = 16$ cells), NR1/NR2B ($n = 36$ cells), NR1/NR2C ($n = 23$ cells) and NR1/NR2D ($n = 15$ cells). Values are mean \pm SD.

NMDAR-mediated responses [42]. Notably, our study showed that resveratrol reduced the increase in intracellular calcium levels induced by NMDA/glycine,

which was applied exogenously. Since resveratrol can modulate intracellular calcium via multiple mechanisms, including calcium release from inositol trisphosphate

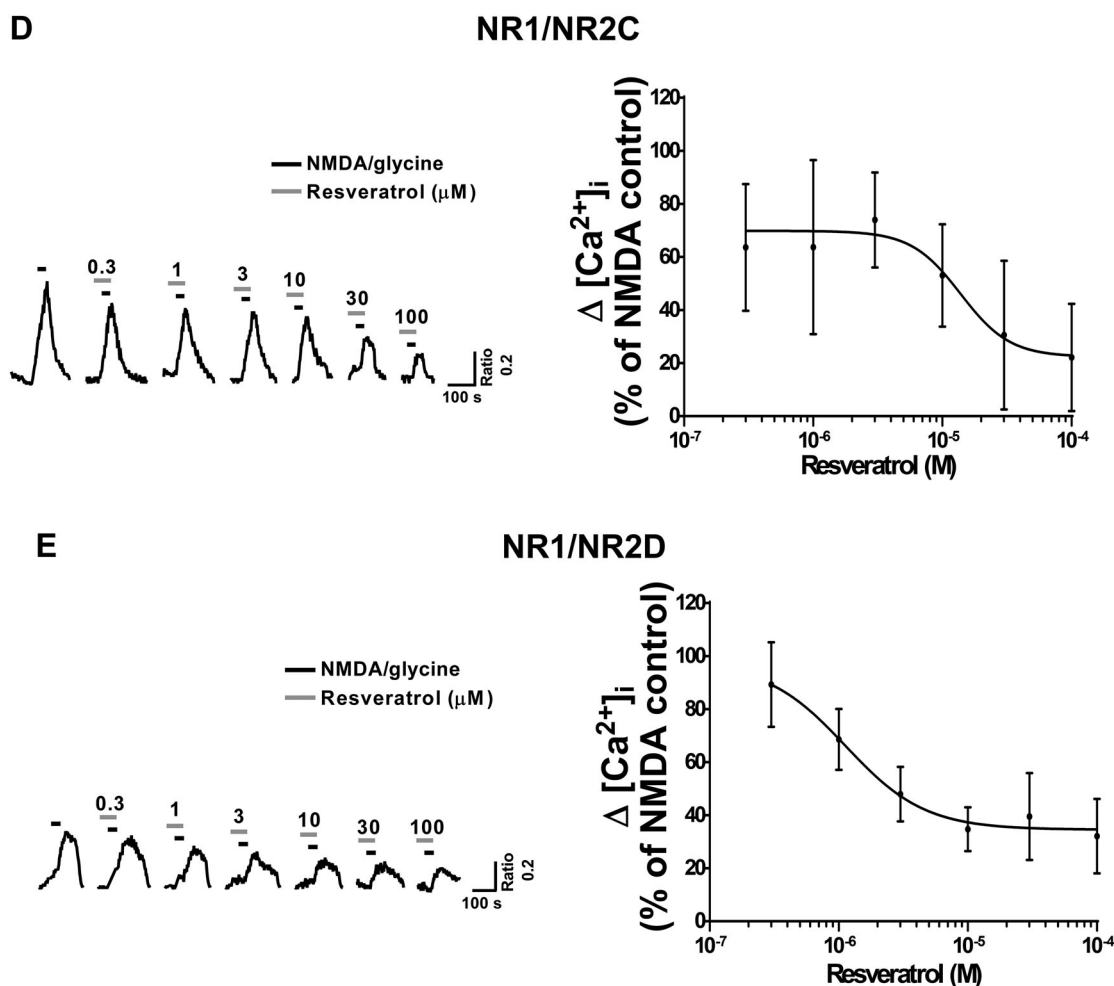


Figure 4 Continued

(IP3) and ryanodine receptors, and calcium influx through plasma membrane ion channels [43]. Thus, the inhibitory action of resveratrol on intracellular calcium levels elicited by NMDA/glycine may not be only due to blockade of NMDAR. In the future, it will determine whether resveratrol can directly inhibit NMDA receptor activity in cortical neurons by patch clamp electrophysiological recording.

Individual NR2 subunits co-assembling with NR1 generate recombinant NMDARs with varying sensitivity to pharmacological agents and channel properties [2]. We further evaluated the effects of resveratrol on the activities of distinct NMDAR subtypes by NMDA-

induced calcium influx in the HEK 293 cell lines with individually stable expression of NR1/NR2A, NR1/NR2B or NR1/NR2C and with transient expression of NR1/NR2D subtypes. Because the transfection efficacy of NR2D was around 10%, the NR1/NR2D-GFP-positive cells were selectively chosen to determine intracellular calcium levels in the present study. Calcium image was also performed in HEK293 expressing NMDAR subtypes with GFP fusion protein which are generated by transient transfection in the previous study [44]. The four NMDAR subtypes exhibit distinct affinity for NMDA. The subtype sensitivity for NMDA-evoked calcium influx was NR2A = NR2B > NR2C > NR2D, which is in accordance with channel properties as previously described [2,45]. Meanwhile, the selective antagonists individually inhibited NMDA-induced calcium influx showing the pharmacological specificity. The four NR2 subtypes also displayed differential sensitivity to resveratrol. Resveratrol exhibited high efficacy to inhibit NR1/NR2B and NR1/NR2C subtypes and high potency for NR1/NR2B and NR1/NR2D. It appears that NR2B is the most sensitive subtype to resveratrol inhibition.

Table 1. Inhibitory effects of resveratrol on NMDA-evoked calcium levels among NMDAR subtypes.

Subtype	IC ₅₀ μM (95% CI)	Hill slope	Inhibitory rate (%)	n
NR1/NR2A	27.1 ± 1.74 (9.01–81.73)	-1.4 ± 0.26	60.3 ± 6.18	16
NR1/NR2B	3.9 ± 1.42 (1.93–7.71)	-1.1 ± 0.19	81.4 ± 2.95	36
NR1/NR2C	25.6 ± 1.35 (14.23–46.17)	-1.6 ± 0.15	79.1 ± 2.37	23
NR1/NR2D	1.1 ± 0.22 (0.40–3.16)	-1.4 ± 0.26	71.9 ± 5.94	15

Note: IC₅₀, half maximal inhibitory concentration.

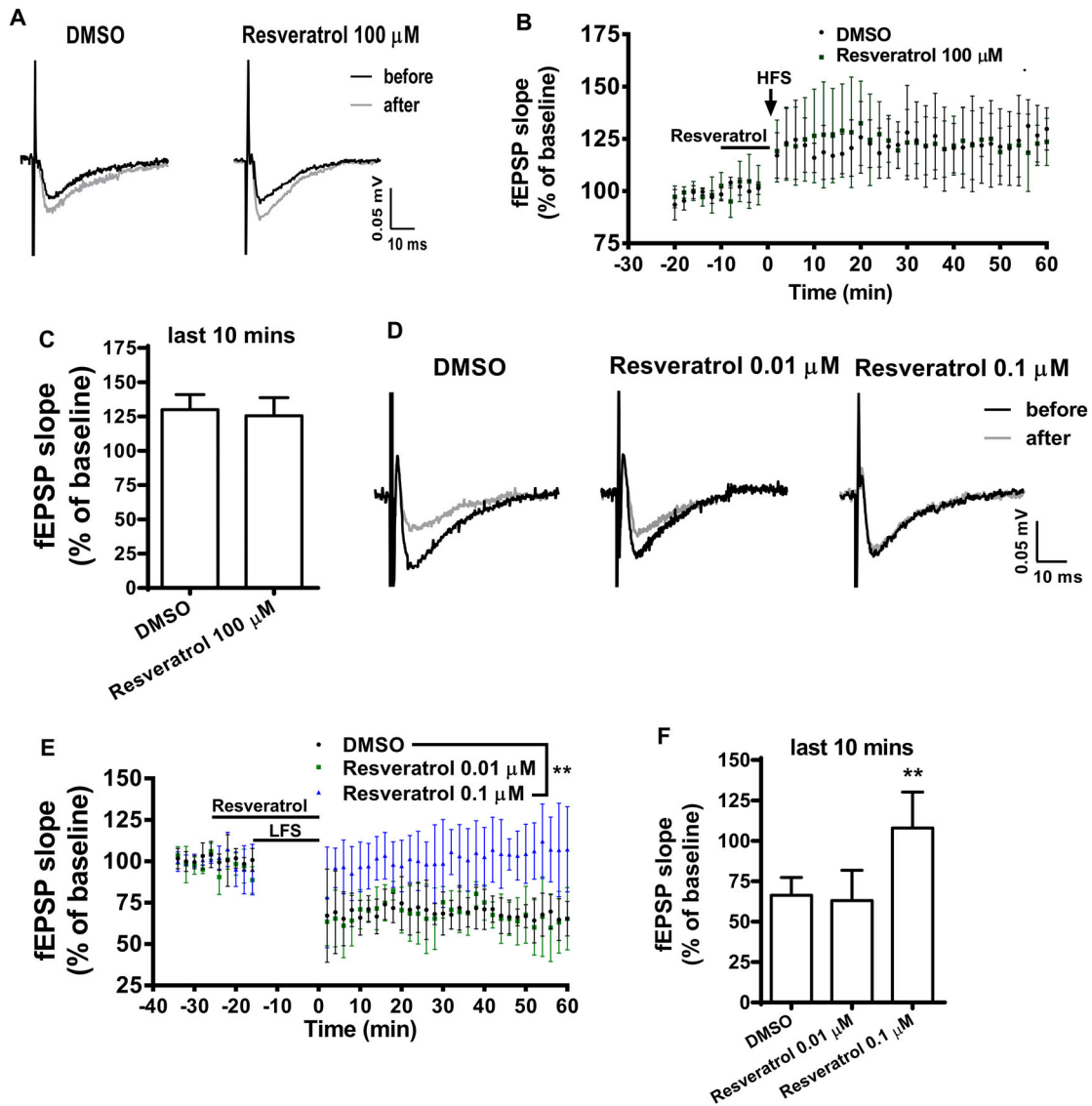


Figure 5. Effects of resveratrol on inductions of LTP and LTD in mouse hippocampal slices. LTP and LTD were individually induced by HFS and LFS in hippocampal schaffer collateral-CA1 synapses. Different concentrations of resveratrol or DMSO was perfused 10 min before and during LFS or HFS. The representative traces of fEPSP before and after HFS (A) and LFS (D) were shown. The average fEPSP slope during the 10–20 min before LTP (B) and LTD (E) induction was taken as baseline, and all values were normalized to this baseline. The averaged fEPSP slope for the last 10 min (51–60 min) during LTP (C) and LTD (F) was quantified and compared. Values are mean \pm SD ($n = 4$ mice). ** $p < .01$ compared with DMSO control.

Resveratrol has a greater inhibitory effect on NMDA-induced calcium influx and neuronal loss at DIV14 comparing to DIV7 in the present study. In a primary cortical neuron, predominant expression of NR2B is observed in the immature neurons at DIV 7 and still maintains in the mature neurons at DIV 21. On the contrary, NR2A is barely detected at DIV 7 and gradually increases from DIV14 to 21 [46]. Thus, the ratio of NR2B/NR2A subunit expression decreased significantly in mature neurons [39]. Consistent with our results, the mature cultures were substantially more sensitive to NMDA toxicity than younger cultures. Notably, the highly selective antagonists of NR1/NR2B receptors exhibited a less

protective effect on NMDA-induced neurotoxicity in mature cells [39]. We observed that resveratrol had a higher inhibitory effect on NR2B subtype than NR2A subtype. Thus, it would expect that NMDA-induced neurotoxicity in immature neurons should be more sensitive to resveratrol. However, our results showed that resveratrol protected NMDA-induced neurotoxicity in mature neurons but not in immature neurons. Activation of intracellular calcium channels including IP3 and ryanodine receptors may involve in the NMDAR-mediated neuronal death [47]. Low level of IP3 and ryanodine receptors are observed in the immature stage and increases in the mature hippocampal and cerebellar

neurons [48,49]. Since resveratrol can inhibit IP3 and ryanodine receptor-mediated intracellular calcium release [43]. Thus, the stronger protective effects of resveratrol in mature neurons might be associated with blockade of intracellular calcium release. Moreover, blockade of both NR2A and NR2B subtypes by resveratrol could reverse NMDA-elicited cell death in mature neurons [8]. Therefore, the inhibitory effects of resveratrol on NMDA-induced calcium response and neurotoxicity in immature and mature stage might consider the modulation of intracellular calcium mobilization in addition to regulation of NR2A and NR2B subtype activity.

NR2B-containing NMDARs play neuropathological roles in stroke, pain, Alzheimer's disease, and drug and alcohol dependency [50–52]. Similar to the NR2B selective antagonists, resveratrol has been shown to protect against stroke, Alzheimer's disease, and neuropathic pain [24,53,54]. In peripheral articular cartilage tissues, NR2B is involved in the production of inflammatory cytokines and pain sensory by mechanotransduction in human osteoarthritic chondrocytes [55], which are reduced by resveratrol in a human subject with mild or moderate knee osteoarthritis [56]. Moreover, resveratrol and NR2B antagonists have been compared and shown similar effects. Injection of resveratrol or NR2B antagonist into lateral ventricle could antagonize the LPS-induced brain inflammation and animal death rate [57]. Accordingly, in addition to antioxidant and anti-inflammatory properties, inhibition of NR2B-containing NMDAR might also contribute to the protective effects of resveratrol on certain diseases associated with NMDAR dysfunction [55,56].

In contrast, resveratrol did not affect solitary tract (NST) NMDAR-mediated baroreflex responses through HPA axis activation [34]. Only high abundant of NR2D and moderate NR2C level are detected in the NST [58] and our results showed that resveratrol has lower inhibitory effects on NR2C and NR2D-containing NMDAR, further support the unique NMDAR subtype-dependent property of resveratrol.

The previous study has indicated that resveratrol at 22 μM did not affect HFS-induced LTP [59]. Consistently, our data further demonstrated that resveratrol at 100 μM could not alter hippocampal LTP elicited by HFS. It is noted that LTP induction depends on high amplitude of NMDAR activation. NR2A-containing NMDARs are required for HFS-induced LTP, but not LFS-evoked LTD in hippocampal slices, whereas induction of LTD but not LTP requires the activation of NR2B-containing NMDARs [7]. Thus, selective inhibition of NMDARs by NR2A antagonists abolished LTP but not LTD induction. In contrast, preferential blockade of NMDARs by NR2B antagonists prevented

LTD induction without affecting LTP production [7]. However, NR2A and NR2B subtypes may both be involved in LTP induction, since NR2B antagonist partially inhibited LTP induction in developing hippocampus with a high ratio of NR2B/2A [60]. Importantly, hippocampal LTP induction may not be altered under partial inhibition of NMDAR activity (less than 40%) either by NR2A or NR2B antagonists or by both in mature animal [61]. Our data show that resveratrol is highly selective for NR2B subtype, but has a much lower inhibitory effect on NR2A subtype. According to the evidence, it suggests that the differential inhibitory efficacy of resveratrol on NMDAR subtypes might be not sufficient to suppress LTP-induced by HFS in the mature hippocampus.

Since NR2B is essential to induce LTD and NR2B antagonists can inhibit LTD induction [7,10,62], the present study revealed that resveratrol suppressed the LTD induction in the hippocampus, in accordance with the preferable inhibitory effect of resveratrol on NR2B-containing NMDAR. It is of note that the increased susceptibility to LTD induction is associated with impaired memory during aging [63,64]. The inhibitory effects of resveratrol on LTD may be involved in its therapeutic potential for age-related cognitive dysfunction.

Our study showed that resveratrol at 0.1 μM was sufficient to inhibit NMDA-induced calcium influx and neuronal loss. Resveratrol at higher concentrations (5–60 μM) has been reported to protect against neuronal death induced by other factors such as MPP⁺, A β and oxygen–glucose deprivation [65]. Acute resveratrol (30 mg/kg; i.p.) treatment can protect the cerebral ischemic injury, whereas the plasma and brain concentration of resveratrol can be detected about 10 μM and 1 μM , respectively [66]. A dose of 10 or 50 mg/kg resveratrol also prevents NMDA-induced seizure response in mice [31], suggesting that resveratrol at 1 μM could inhibit NMDA-evoked neuronal activity in vivo. In the clinical study, oral resveratrol with 250 or 500 mg increases cerebral blood flow during a cognitive task and the peak plasma concentration is around 1–2 μM [67]. Therefore, the therapeutic dosage of resveratrol should be implicated on NMDAR-mediated responses.

In summary, our data demonstrate that resveratrol produced differential inhibitory effects on NMDA-induced excitotoxicity and NMDA-induced calcium influx in immature and mature cortical neurons. In HEK 293 cells with different expression of individual NR2 subunits, resveratrol inhibited NMDAR activity dependent on the NR2 subunit, with preferable to NR2B-containing NMDAR. Moreover, resveratrol specifically decreased the induction of LTD, but not LTP in mouse hippocampal slices. Despite encouraging

data from animal studies, NR2B-selective antagonists have not succeeded in clinical trials yet because of uncertain biosafety and pharmacokinetic profiles. Resveratrol is considered a dietary supplement and its safety has also been confirmed [68]. Resveratrol is promising in health promotion, not only for its antioxidant activities but also for its anti-inflammatory and neuroprotective properties. The unique NMDAR subtype inhibitory properties of resveratrol we revealed in the present study provide more evidence to support its potential implication in the treatment of the neurological disorders associated with hyperfunction of NMDARs, in particular, NR2B subunit-containing NMDARs.

Acknowledgements

The authors thank Dr Chia-Hsiang Chen (Chang Gung Memorial Hospital) for providing the vectors with the cDNA of NMDAR subtypes and Dr A-Min Huang (National Cheng-Kung University) for offering the lentiviral related plasmid DNA. C. P. H., H. H. C., M. H. C. conceived the study and are responsible for experimental design; C. P. H. performed cell MTT, calcium image, electrophysiology experiments and data analysis; L. C. participated in the neuronal culture; W. T. C. prepared cells expressing NMDAR; C. P. H. prepared the figures and drafted the manuscript; M. H. C., H. H. C. edited the manuscript.

Disclosure statement

No potential conflict of interest was reported by the authors.

Funding

This work was supported by National Health Research Institutes [grant number NP-106-PP05].

Ethics approval

All experiments in animal studies were approved by Institutional Animal Care and Use Committee of the National Health Research Institutes (NHRI-IACUC-102038-A).

ORCID

Hwei-Hsien Chen  <http://orcid.org/0000-0002-8509-6448>
Ming-Huan Chan  <http://orcid.org/0000-0003-3206-8731>

References

- [1] Traynelis SF, Wollmuth LP, McBain CJ, Menniti FS, Vance KM, Ogden KK, et al. Glutamate receptor ion channels: structure, regulation, and function. *Pharmacol Rev*. 2010 Sep;62(3):405–96.
- [2] Paoletti P, Bellone C, Zhou Q. NMDA receptor subunit diversity: impact on receptor properties, synaptic plasticity and disease. *Nat Rev Neurosci*. 2013 Jun;14(6):383–400.
- [3] Cull-Candy SG, Leszkiewicz DN. Role of distinct NMDA receptor subtypes at central synapses. *Sci STKE*. 2004 Oct 19;2004(255):re16.
- [4] Cull-Candy S, Brickley S, Farrant M. NMDA receptor subunits: diversity, development and disease. *Curr Opin Neurobiol*. 2001 Jun;11(3):327–35.
- [5] Sanz-Clemente A, Nicoll RA, Roche KW. Diversity in NMDA receptor composition: many regulators, many consequences. *Neuroscientist*. 2013 Feb;19(1):62–75.
- [6] Liu Y, Wong TP, Aarts M, Rooyackers A, Liu L, Lai TW, et al. NMDA receptor subunits have differential roles in mediating excitotoxic neuronal death both in vitro and in vivo. *J Neurosci*. 2007 Mar 14;27(11):2846–57.
- [7] Liu L, Wong TP, Pozza MF, Lingenhoehl K, Wang Y, Sheng M, et al. Role of NMDA receptor subtypes in governing the direction of hippocampal synaptic plasticity. *Science*. 2004 May 14;304(5673):1021–4.
- [8] von Engelhardt J, Coserea I, Pawlak V, Fuchs EC, Kohr G, Seeburg PH, et al. Excitotoxicity in vitro by NR2A- and NR2B-containing NMDA receptors. *Neuropharmacology*. 2007 Jul;53(1):10–7.
- [9] Kohr G, Jensen V, Koester HJ, Mihajlovic AL, Utvik JK, Kvello A, et al. Intracellular domains of NMDA receptor subtypes are determinants for long-term potentiation induction. *J Neurosci*. 2003 Nov 26;23(34):10791–9.
- [10] Massey PV, Johnson BE, Moulton PR, Auberson YP, Brown MW, Molnar E, et al. Differential roles of NR2A and NR2B-containing NMDA receptors in cortical long-term potentiation and long-term depression. *J Neurosci*. 2004 Sep 8;24(36):7821–8.
- [11] Gladding CM, Raymond LA. Mechanisms underlying NMDA receptor synaptic/extrasynaptic distribution and function. *Mol Cell Neurosci*. 2011 Dec;48(4):308–20.
- [12] Hatton CJ, Paoletti P. Modulation of triheteromeric NMDA receptors by N-terminal domain ligands. *Neuron*. 2005 Apr 21;46(2):261–74.
- [13] Lai TW, Shyu WC, Wang YT. Stroke intervention pathways: NMDA receptors and beyond. *Trends Mol Med*. 2011 May;17(5):266–75.
- [14] Milnerwood AJ, Gladding CM, Pouladi MA, Kaufman AM, Hines RM, Boyd JD, et al. Early increase in extrasynaptic NMDA receptor signaling and expression contributes to phenotype onset in Huntington's disease mice. *Neuron*. 2010 Jan 28;65(2):178–90.
- [15] Ronicke R, Mikhaylova M, Ronicke S, Meinhardt J, Schroder UH, Fandrich M, et al. Early neuronal dysfunction by amyloid beta oligomers depends on activation of NR2B-containing NMDA receptors. *Neurobiol Aging*. 2011 Dec;32(12):2219–28.
- [16] Qiu S, Li XY, Zhuo M. Post-translational modification of NMDA receptor GluN2B subunit and its roles in chronic pain and memory. *Semin Cell Dev Biol*. 2011 Jul;22(5):521–9.
- [17] Yuan H, Myers SJ, Wells G, Nicholson KL, Swanger SA, Lyuboslavsky P, et al. Context-dependent GluN2B-selective inhibitors of NMDA receptor function are neuroprotective with minimal side effects. *Neuron*. 2015 Mar 18;85(6):1305–18.

- [18] Hu NW, Klyubin I, Anwyl R, Rowan MJ. Glun2b subunit-containing NMDA receptor antagonists prevent Abeta-mediated synaptic plasticity disruption in vivo. *Proc Natl Acad Sci U S A*. 2009 Dec 1;106(48):20504–9.
- [19] Salter MG, Fern R. NMDA receptors are expressed in developing oligodendrocyte processes and mediate injury. *Nature*. 2005 Dec 22;438(7071):1167–71.
- [20] Doyle S, Hansen DB, Vella J, Bond P, Harper G, Zammit C, et al. Vesicular glutamate release from central axons contributes to myelin damage. *Nat Commun*. 2018 Mar 12;9(1):1032.
- [21] Chizh BA, Headley PM, Tzschentke TM. NMDA receptor antagonists as analgesics: focus on the NR2B subtype. *Trends Pharmacol Sci*. 2001 Dec;22(12):636–42.
- [22] Albenis BC, Igoeche C, Janigro D, Ilkanich E. Why do many NMDA antagonists fail, while others are safe and effective at blocking excitotoxicity associated with dementia and acute injury? *Am J Alzheimers Dis Other Demen*. 2004 Sep-Oct;19(5):269–74.
- [23] Mullin GE. Red wine, grapes, and better health—resveratrol. *Nutr Clin Pract*. 2011 Dec;26(6):722–3.
- [24] Shetty AK. Promise of resveratrol for easing status epilepticus and epilepsy. *Pharmacol Ther*. 2011 Sep;131(3):269–86.
- [25] Lopez MS, Dempsey RJ, Vemuganti R. Resveratrol neuroprotection in stroke and traumatic CNS injury. *Neurochem Int*. 2015 Oct;89:75–82.
- [26] Pervaiz S, Holme AL. Resveratrol: its biologic targets and functional activity. *Antioxid Redox Signal*. 2009 Nov;11(11):2851–97.
- [27] Yanez M, Galan L, Matias-Guiu J, Vela A, Guerrero A, Garcia AG. CSF from amyotrophic lateral sclerosis patients produces glutamate independent death of rat motor brain cortical neurons: protection by resveratrol but not riluzole. *Brain Res*. 2011 Nov 14;1423:77–86.
- [28] Chen J, Bai Q, Zhao Z, Sui H, Xie X. Resveratrol improves delayed r-tPA treatment outcome by reducing MMPs. *Acta Neurol Scand*. 2016 Jul;134(1):54–60.
- [29] Zhang LN, Hao L, Wang HY, Su HN, Sun YJ, Yang XY, et al. Neuroprotective effect of resveratrol against glutamate-induced excitotoxicity. *Adv Clin Exp Med*. 2015 Jan-Feb;24(1):161–5.
- [30] Gao ZB, Chen XQ, Hu GY. Inhibition of excitatory synaptic transmission by trans-resveratrol in rat hippocampus. *Brain Res*. 2006 Sep 21;1111(1):41–7.
- [31] Wang YJ, Hsieh CP, Chan MH, Chan TY, Chen L, Chen HH. Distinct effects of resveratrol on seizures and hyperexcitability induced by NMDA and 4-aminopyridine. *Nutr Neurosci*. 2018 Apr 12:1–11.
- [32] Takehana S, Kubota Y, Uotsu N, Yui K, Iwata K, Shimazu Y, et al. The dietary constituent resveratrol suppresses nociceptive neurotransmission via the NMDA receptor. *Mol Pain*. 2017 Jan;13:1744806917697010.
- [33] Yang X, Si P, Qin H, Yin L, Yan LJ, Zhang C. The neuroprotective effects of SIRT1 on NMDA-induced excitotoxicity. *Oxid Med Cell Longev*. 2017;2017:2823454.
- [34] Knutson N, Wood CE. Interaction of PGHS-2 and glutamatergic mechanisms controlling the ovine fetal hypothalamus-pituitary-adrenal axis. *Am J Physiol Regul Integr Comp Physiol*. 2010 Jul;299(1):R365–70.
- [35] Ichikawa M, Muramoto K, Kobayashi K, Kawahara M, Kuroda Y. Formation and maturation of synapses in primary cultures of rat cerebral cortical cells: an electron microscopic study. *Neurosci Res*. 1993 Feb;16(2):95–103.
- [36] Schubert D, Piasecki D. Oxidative glutamate toxicity can be a component of the excitotoxicity cascade. *J Neurosci*. 2001 Oct 1;21(19):7455–62.
- [37] France G, Fernandez-Fernandez D, Burnell ES, Irvine MW, Monaghan DT, Jane DE, et al. Multiple roles of GluN2B-containing NMDA receptors in synaptic plasticity in juvenile hippocampus. *Neuropharmacology*. 2017 Jan;112(Pt A):76–83.
- [38] Xiao L, Hu C, Feng C, Chen Y. Switching of N-methyl-D-aspartate (NMDA) receptor-favorite intracellular signal pathways from ERK1/2 protein to p38 mitogen-activated protein kinase leads to developmental changes in NMDA neurotoxicity. *J Biol Chem*. 2011 Jun 10;286(23):20175–93.
- [39] Sinor JD, Du S, Venneti S, Blitzblau RC, Leszkiewicz DN, Rosenberg PA, et al. NMDA and glutamate evoke excitotoxicity at distinct cellular locations in rat cortical neurons in vitro. *J Neurosci*. 2000 Dec 1;20(23):8831–7.
- [40] Wang YJ, Chan MH, Chen L, Wu SN, Chen HH. Resveratrol attenuates cortical neuron activity: roles of large conductance calcium-activated potassium channels and voltage-gated sodium channels. *J Biomed Sci*. 2016 May 21;23(1):47.
- [41] McCalley AE, Kaja S, Payne AJ, Koulen P. Resveratrol and calcium signaling: molecular mechanisms and clinical relevance. *Molecules*. 2014 Jun 5;19(6):7327–40.
- [42] Stanika RI, Villanueva I, Kazanina G, Andrews SB, Pivovarov NB. Comparative impact of voltage-gated calcium channels and NMDA receptors on mitochondria-mediated neuronal injury. *J Neurosci*. 2012 May 9;32(19):6642–50.
- [43] Carrasco-Pozo C, Pastene E, Vergara C, Zapata M, Sandoval C, Gotteland M. Stimulation of cytosolic and mitochondrial calcium mobilization by indomethacin in Caco-2 cells: modulation by the polyphenols quercetin, resveratrol and rutin. *Biochim Biophys Acta*. 2012 Dec;1820(12):2052–61.
- [44] Adamusova E, Cais O, Vyklicky V, Kudova E, Chodounska H, Horak M, et al. Pregnenolone sulfate activates NMDA receptor channels. *Physiol Res*. 2013;62(6):731–6.
- [45] Domingues AM, Neugebauer KM, Fern R. Identification of four functional NR3B isoforms in developing white matter reveals unexpected diversity among glutamate receptors. *J Neurochem*. 2011 May;117(3):449–60.
- [46] Li JH, Wang YH, Wolfe BB, Krueger KE, Corsi L, Stocca G, et al. Developmental changes in localization of NMDA receptor subunits in primary cultures of cortical neurons. *Eur J Neurosci*. 1998 May;10(5):1704–15.
- [47] Ruiz A, Matute C, Alberdi E. Endoplasmic reticulum Ca²⁺ release through ryanodine and IP(3) receptors contributes to neuronal excitotoxicity. *Cell Calcium*. 2009 Oct;46(4):273–81.
- [48] Genazzani AA, Carafoli E, Guerini D. Calcineurin controls inositol 1,4,5-trisphosphate type 1 receptor expression in neurons. *Proc Natl Acad Sci U S A*. 1999 May 11;96(10):5797–801.
- [49] Wayman GA, Yang D, Bose DD, Lesiak A, Ledoux V, Bruun D, et al. PCB-95 promotes dendritic growth via

- ryanodine receptor-dependent mechanisms. *Environ Health Perspect.* 2012 Jul;120(7):997–1002.
- [50] Chazot PL. The NMDA receptor NR2B subunit: a valid therapeutic target for multiple CNS pathologies. *Curr Med Chem.* 2004 Feb;11(3):389–96.
- [51] deBacker J, Hawken ER, Normandeau CP, Jones AA, Di Prospero C, Mechefske E, et al. GluN2B-containing NMDA receptors blockade rescues bidirectional synaptic plasticity in the bed nucleus of the stria terminalis of cocaine self-administering rats. *Neuropsychopharmacology.* 2015 Jan;40(2):394–405.
- [52] Wang J, Carnicella S, Phamluong K, Jeanblanc J, Ronesi JA, Chaudhri N, et al. Ethanol induces long-term facilitation of NR2B-NMDA receptor activity in the dorsal striatum: implications for alcohol drinking behavior. *J Neurosci.* 2007 Mar 28;27(13):3593–602.
- [53] Robb EL, Stuart JA. trans-Resveratrol as a neuroprotectant. *Molecules.* 2010 Mar 3;15(3):1196–212.
- [54] Tao L, Ding Q, Gao C, Sun X. Resveratrol attenuates neuropathic pain through balancing pro-inflammatory and anti-inflammatory cytokines release in mice. *Int Immunopharmacol.* 2016 May;34:165–72.
- [55] Ramage L, Martel MA, Hardingham GE, Salter DM. NMDA receptor expression and activity in osteoarthritic human articular chondrocytes. *Osteoarthritis Cartilage.* 2008 Dec;16(12):1576–84.
- [56] Marouf BH, Hussain SA, Ali ZS, Ahmmad RS. Resveratrol supplementation reduces pain and inflammation in knee osteoarthritis patients treated with Meloxicam: A randomized placebo-controlled study. *J Med Food.* 2018 Aug 30;21(12):1253–59.
- [57] Imamura Y, Yoshikawa N, Murkami Y, Mitani S, Matsumoto N, Matsumoto H, et al. Effect of histone acetylation on N-methyl-D-aspartate 2B receptor subunits and interleukin-1 receptors in association with nociception-related somatosensory cortex dysfunction in a mouse model of sepsis. *Shock.* 2016 Jun;45(6):660–7.
- [58] Guthmann A, Herbert H. Expression of N-methyl-D-aspartate receptor subunits in the rat parabrachial and Kolliker-Fuse nuclei and in selected pontomedullary brainstem nuclei. *J Comp Neurol.* 1999 Dec 27;415(4):501–17.
- [59] Wang R, Zhang Y, Li J, Zhang C. Resveratrol ameliorates spatial learning memory impairment induced by Abeta1-42 in rats. *Neuroscience.* 2017 Mar 6;344:39–47.
- [60] Bartlett TE, Bannister NJ, Collett VJ, Dargan SL, Massey PV, Bortolotto ZA, et al. Differential roles of NR2A and NR2B-containing NMDA receptors in LTP and LTD in the CA1 region of two-week old rat hippocampus. *Neuropharmacology.* 2007 Jan;52(1):60–70.
- [61] Berberich S, Punnakkal P, Jensen V, Pawlak V, Seeburg PH, Hvalby O, et al. Lack of NMDA receptor subtype selectivity for hippocampal long-term potentiation. *J Neurosci.* 2005 Jul 20;25(29):6907–10.
- [62] Shipton OA, Paulsen O. Glun2a and GluN2B subunit-containing NMDA receptors in hippocampal plasticity. *Philos Trans R Soc Lond B Biol Sci.* 2014 Jan 5;369(1633):20130163.
- [63] Foster TC. Involvement of hippocampal synaptic plasticity in age-related memory decline. *Brain Res Brain Res Rev.* 1999 Nov;30(3):236–49.
- [64] Malenka RC, Bear MF. LTP and LTD: an embarrassment of riches. *Neuron.* 2004 Sep 30;44(1):5–21.
- [65] Zhang F, Liu J, Shi JS. Anti-inflammatory activities of resveratrol in the brain: role of resveratrol in microglial activation. *Eur J Pharmacol.* 2010 Jun 25;636(1–3):1–7.
- [66] Wang Q, Xu J, Rottinghaus GE, Simonyi A, Lubahn D, Sun GY, et al. Resveratrol protects against global cerebral ischemic injury in gerbils. *Brain Res.* 2002 Dec 27;958(2):439–47.
- [67] Kennedy DO, Wightman EL, Reay JL, Lietz G, Okello EJ, Wilde A, et al. Effects of resveratrol on cerebral blood flow variables and cognitive performance in humans: a double-blind, placebo-controlled, crossover investigation. *Am J Clin Nutr.* 2010 Jun;91(6):1590–7.
- [68] Almeida L, Vaz-da-Silva M, Falcao A, Soares E, Costa R, Loureiro AI, et al. Pharmacokinetic and safety profile of trans-resveratrol in a rising multiple-dose study in healthy volunteers. *Mol Nutr Food Res.* 2009 May;53(Suppl 1):S7–15.